Supporting Information

Ascorbic Acid-Enhanced MOF-Derived CeO_2 for Improved Substrate Selectivity in Glucose Detection

*Yameng Xie[a], Jiayu Huang[a], Yunjian Ye[a], Hengrui Ma[a], Xiqing Cheng[b], Qin Kuang[a,c]**

[a]State Key Laboratory of Physical Chemistry of Solid Surfaces, Collaborative Innovation Center of Chemistry for Energy Materials, Department of Chemistry, College of Chemistry and Chemical Engineering, Xiamen University, Xiamen, 361005, China

[b]School of Chemical and Environmental Engineering, Shanghai Institute of Technology, Shanghai, 201418, China

[c]Innovation Laboratory for Sciences and Technologies of Energy Materials of Fujian Province (IKKEM), Xiamen 361005, China

*Corresponding author E-mail: qkuang@xmu.edu.cn

Experimental Section

Chemicals and materials. All chemical reagents were used as received without further purification. 3,3′,5,5′ tetramethylbenzidine (TMB) were obtained from Alfa Aesar. 1,3,5-Benzenetricarboxylic were gained from TCI. Ascorbic acid (AA), Zinc nitrate hexahydrate ($Zn(NO_3)_2 \cdot 6H_2O$), Magnesium chloride ($MgCl_2$), cerium nitrate hexahydrate ($Ce(NO_3)_3 \cdot 6H_2O$), nickel (II) nitrate hexahydrate ($Ni(NO_3)_2 \cdot 6H_2O$), acetic acid ($C_2H_4O_2$), sodium acetate (NaAc), hydrogen peroxide (H_2O_2, 30%), sodium chloride (NaCl), potassium chloride (KCl), D-(+)-glucose anhydrous ($C_6H_{12}O_6$, glucose), sucrose ($C_{12}H_{22}O_{11}$), L-proline ($C_5H_9NO_2$, Pro) and dimethyl sulfoxide (C_2H_6OS, DMSO) were purchased from Sinopharm Chemical Reagent Co. Ltd (Shanghai, China). Tyrosinase (TYR), lysozyme, and trypsin were purchased from Sigma-Aldrich. 5, 5′-dimethyl-1-pyrroline-oxide (DMPO) was obtained from Energy Chemical (Shanghai, China). Bicinchoninic acid (BCA) protein assay kit was obtained from Beyotime. Human serum was purchased from Lablead. All solutions were prepared with ultrapure water obtained from a Barnstead Nanopure Water System.

Synthesis of CeBTC and CeO_2. The sacrificial precursor CeBTC was synthesized by means of a modified method.[20] Typically, a solution containing 2.1 g of 1,3,5-benzenetricarboxylic acid (H_3BTC), 10 mL of H_2O and 10 mL of ethanol was heated to 60 °C. And then 45 mL of water containing 4.34 g of Ce $(NO_3)_3 \cdot 6H_2O$ was added to above resulting solution under vigorous stirring. After 1 h, the precipitate was

collected by filtration and washed with ethanol and water for several times. Finally, the yellow solid was dried at 70 °C for 8 h, and treated at 200 °C, 350 °C or 500 °C under air for 2 h, respectively. The obtained samples were named CeBTC-200, CeO_2-350 and CeO_2-500 based on different treatment temperatures.

Synthesis of CeO_2-350-AA. First, the as-prepared CeO_2-350 (50 mg) were dispersed in distilled water (16 mL) and AA (25 mg, 0.5 mL) was added, followed by vigorous stirring for 3 h at room temperature. The resulting suspension was collected by centrifugation at 8,500 rpm, washed four times with distilled water, and dried under 60 °C overnight. The product obtained was denoted as CeO_2-350-AA.

Synthesis of CeO_2-350-$NaBH_4$. The as-prepared CeO_2-350 (50 mg) were dispersed in distilled water (16 mL) and $NaBH_4$ (5.5 mg, 0.5 mL) was added, followed by vigorous stirring for 3 h at room temperature. The resulting suspension was collected by centrifugation at 8,500 rpm, washed four times with water, and dried under 60 °C overnight. The product obtained was denoted as CeO_2-350-$NaBH_4$.

Synthesis of CeO_2-H_2. The as-prepared CeO_2-350 power was transferred into a ceramic boat and heated to 350 °C, 500 °C or 700 °C for 2 hours with a heating rate of 5 °C min^{-1} under Ar/H_2, followed by natural cooling to room temperature. The obtained samples were named CeO_2-350-H_2, CeO_2-500-H_2 and CeO_2-700-H_2 based on different treatment temperatures.

Synthesis of GOx@CeO_2-350-AA. The 5 mg GOx was dissolved in 2 mL deionized water and 10 mg CeO_2-350 in 2 mL water. After mixing and stirring for 3 h, the

supernatant was removed after centrifugation at 8500 rpm for 2 min, and the GOx@CeO_2-350-AA were dissolved in 1 mL deionized water and stored at 5 ° C.

Characterization of samples. The morphologies of the samples were viewed by field emission scanning electron microscopy (FE-SEM, HITACHI-S4800, Japan), and high-angle annular dark-field scanning TEM (HAADF-STEM) was obtained by transmission electron microscopy (TEM, Tecnai F30, USA, 300 kV). The crystallinity was investigated by powder X-ray diffraction (XRD, Ultima IV) using Cu Kα radiation at λ = 1.5418 Å, 40 kV, and 40 mA. X-ray photoelectron spectroscopy (XPS) was performed on a PHI Quantum-2000 spectrometer. Thermal gravimetric analysis (TG) was conducted on TA instrument (Q600 SDT, USA) from room temperature to 800 °C under N_2 atmosphere. The hydroxyl radical signals were collected by electron spin resonance (ESR) spectrometry (Bruker X-band A200, German). The Fourier transform infrared (FT-IR) spectra were obtained by using a Thermo Nicolet 380 spectrophotometer. The absorption spectra of steady-state kinetic measurements were collected on a Shimadzu UV-2550 spectrophotometer (Shimadzu, Japan). Tecan Safire2 Multi-Mode Microplate Reader was employed for other colorimetric measurements.

The POD-like catalytic activities. The experiments were conducted on 96-well plates for four times confirmed on TMB substrates. To confirm the POD-like activity, TMB (10 μL, 10 mM), H_2O_2 (10 μL, 1 M) and CeO_2 (10 μL, 1 mg mL^{-1}) were successively added into acetate buffer solution (190 μL, pH=4), and the absorbance

profiles were then recorded at 652 nm by a multi-mode microplate reader after 10 min reaction.

The detection of intermediates. The •OH intermediates produced during the POD-like reaction was monitored by ESR under the experimental conditions using DMPO as a spin trap.

Steady-state kinetic measurements. The steady-state kinetic measurements of POD-like nanozymes based on CeO_2-350 and CeO_2-350-AA were conducted by recording the absorbance at 652 nm. To this end, different concentrations of TMB/ H_2O_2 were first added into acetate buffer (1600 μL) followed by CeO_2-350/ CeO_2-350-AA (80 μL, 1 mg mL^{-1}). The absorbance A of each solution was recorded immediately. The resulting substrate concentration-dependent reaction rate curves were then fitted according to the Michaelis-Menten model. The maximum reaction rate (ν_{max}) and Michaelis-Menten constant (K_m) were calculated using Lineweaver-Burk plot (double-reciprocal plot) shown in Eq. (1):

$$1/\nu = K_m/\nu_{max} \times 1/[S] + 1/\nu_{max} \qquad (1)$$

where ν is the initial velocity and [S] represents the concentration of TMB.

Detection of glucose. The liquid-phase glucose biosensing system was established via combining the GOx and POD-like nanozyme. In detail, different concentrations of glucose (50 μL) were added into acetate buffer (870 μL) followed by GOx@CeO_2-350-AA (40 μL), TMB (40 μL, 10 mM). After incubation at room temperature for 10

min, the absorbance of the biosensing system were detected by 652 nm to determine the linear detection interval and the limit of detection (LOD) of the glucose biosensing system. The LOD was calculated by the following equation:

$$LOD = KS_b/s \qquad (1)$$

K is a constant value of 3, S_b is the standard deviation of 20 measurements, and s is the slope of the standard curve. The kinetics of the chromogenic reaction were investigated by recording the absorption spectra from 800 nm to 500 nm each 5 min.

Determination of loading amount of GOx on CeO_2-350-AA. We measured the protein contents of both the original GOx solution and the supernatant obtained after physical adsorption and centrifugation using the BCA protein assay kit, respectively. The loading amount of GOx on CeO_2-350-AA was calculated by subtracting the GOx content in the supernatant from the initial GOx amount.

Interference study. To measure the anti-interference ability of the GOx@CeO_2-350-AA nanozymes + TMB system, a series of potential interfering substrates were chosen for testing. 5-fold concentrations of potential interfering substrates, including natural enzymes (CAT, lysozyme, trypsin, lipase) metal irons (Na^+, K^+, Mg^{2+}, Zn^{2+}, Ni^{2+}), sugars (sucrose), and amino acid (L-proline, L-isoleucine, glycine) were added into the GOx@CeO_2-350-AA + TMB system. The absorbance values at 652 nm were recorded to compare the interference effect.

Supplementary Results

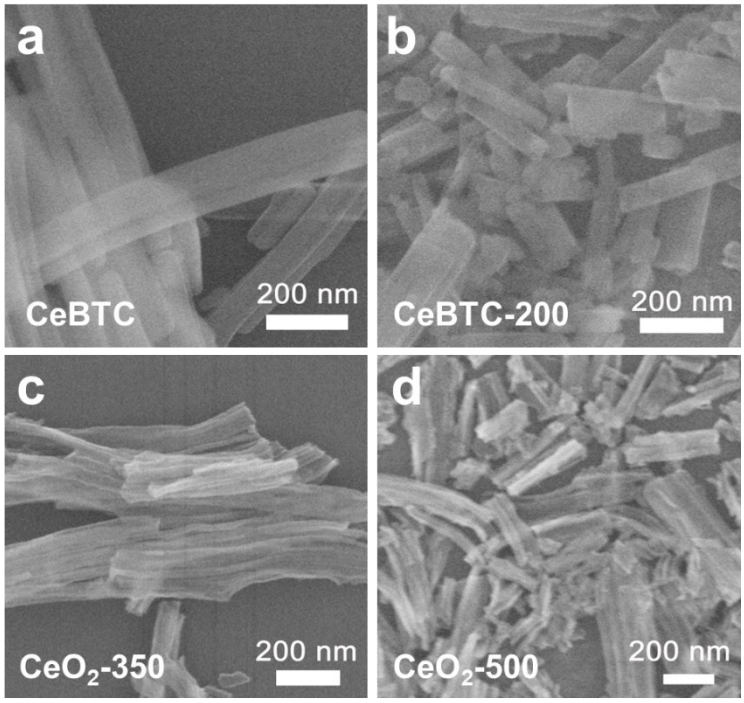

Figure S1. SEM images of (a) CeBTC, (b) CeBTC-200, (c) CeO_2-350, and (d) CeO_2-500.

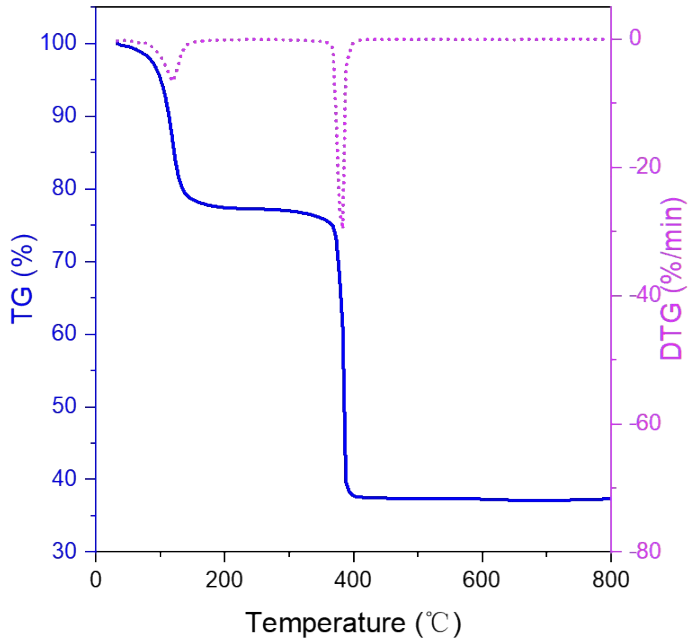

Figure S2. TG and DTG curves of CeBTC under N_2 flow.

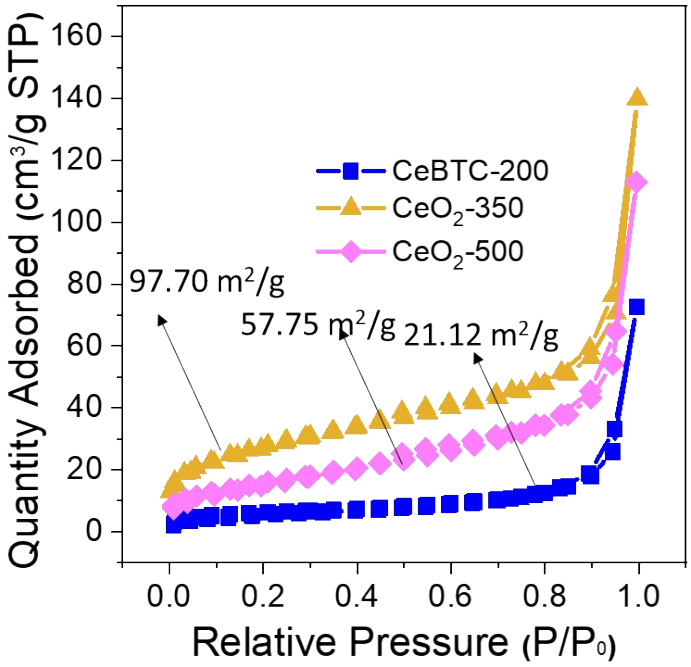

Figure S3. BET analysis of CeBTC-200, CeO_2-350 and CeO_2-500.

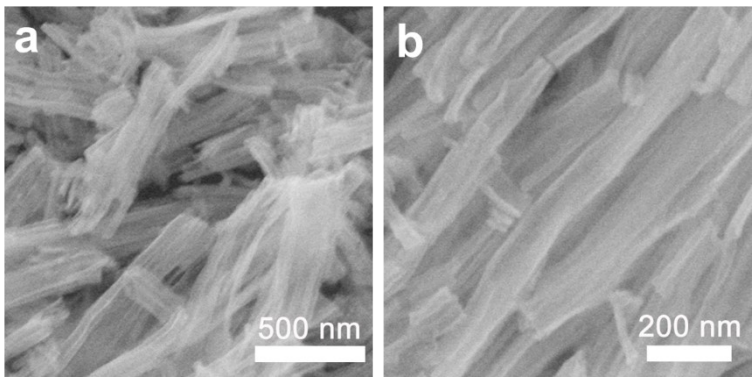

Figure S4. SEM images of CeO_2-350-AA.

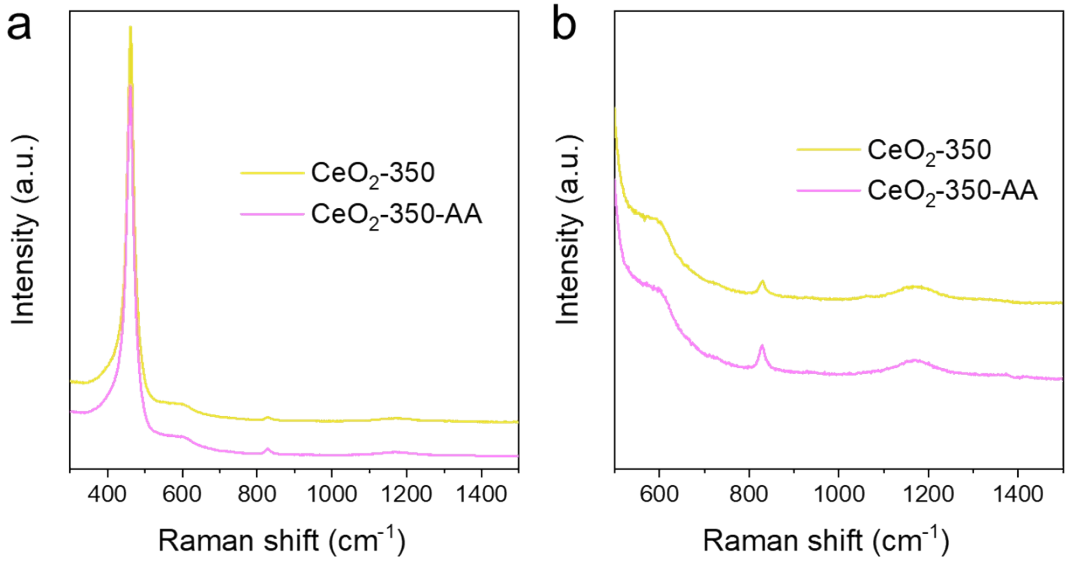

Figure S5. Raman spectra of CeO_2-350 and CeO_2-350-AA.

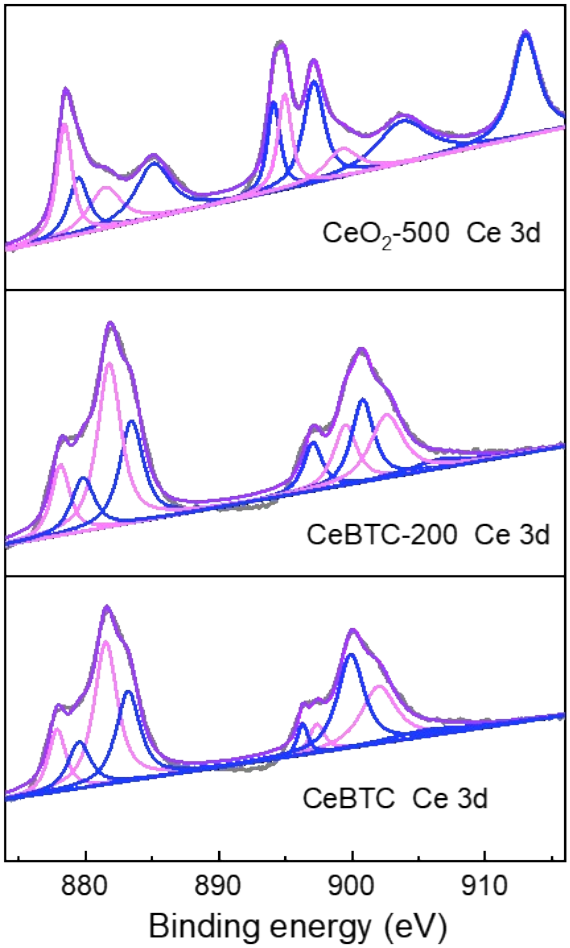

Figure S6. High-resolution XPS spectra of Ce 3d.

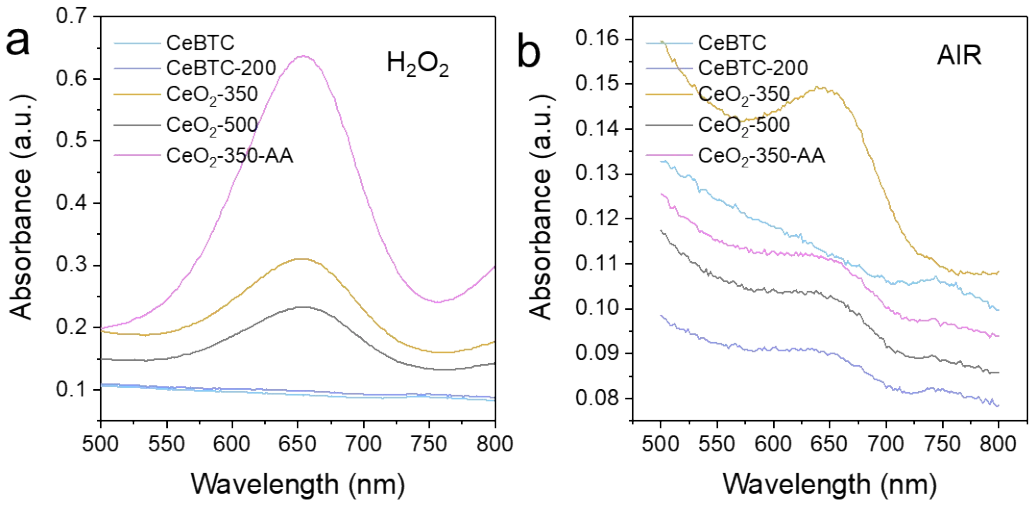

Figure S7. UV-vis of (a) peroxidase-like and (b) oxidase-like activities of CeBTC and its derivatives.

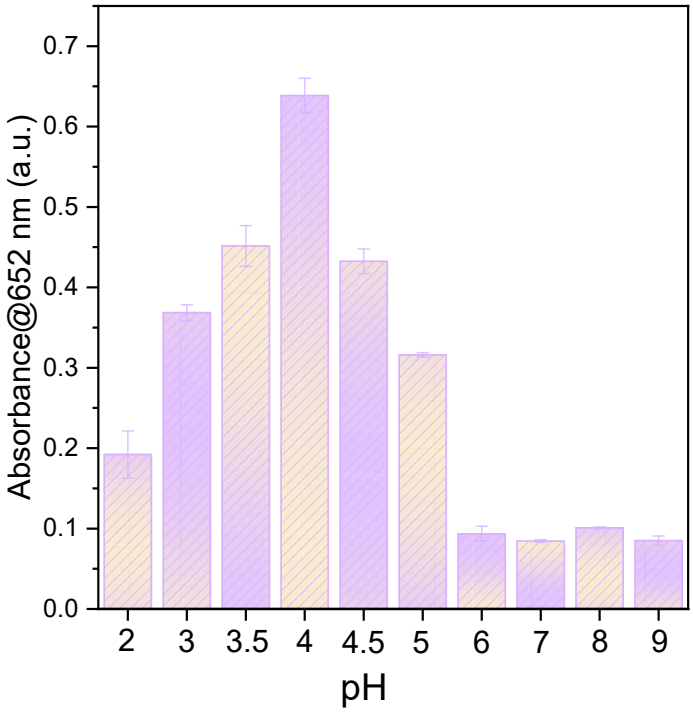

Figure S8. Influence of pH on the peroxidase-like activity of CeO_2-350-AA.

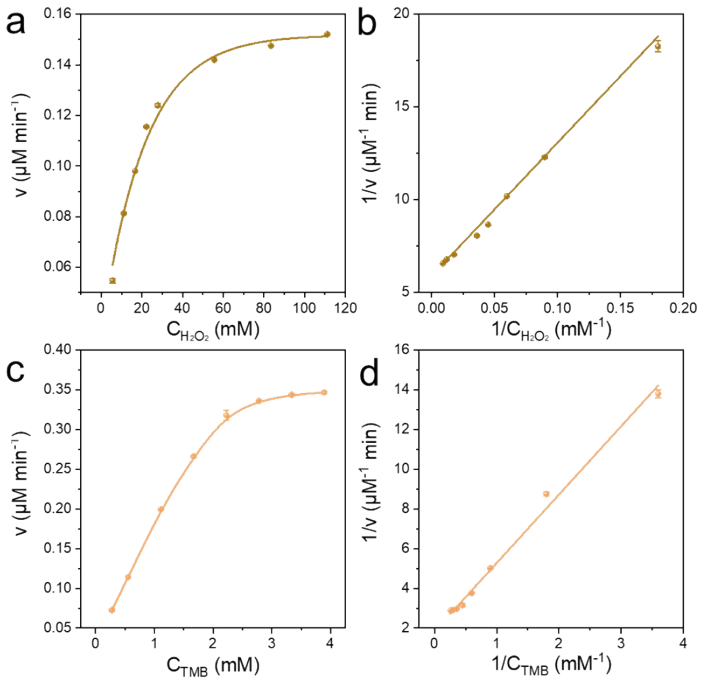

Figure S9. (a) Steady-state kinetic assay and (b) Michaelis-Menten curves toward H_2O_2 of CeO_2-350. (c) Steady-state kinetic assay and (d) Michaelis-Menten curves toward TMB of CeO_2-350.

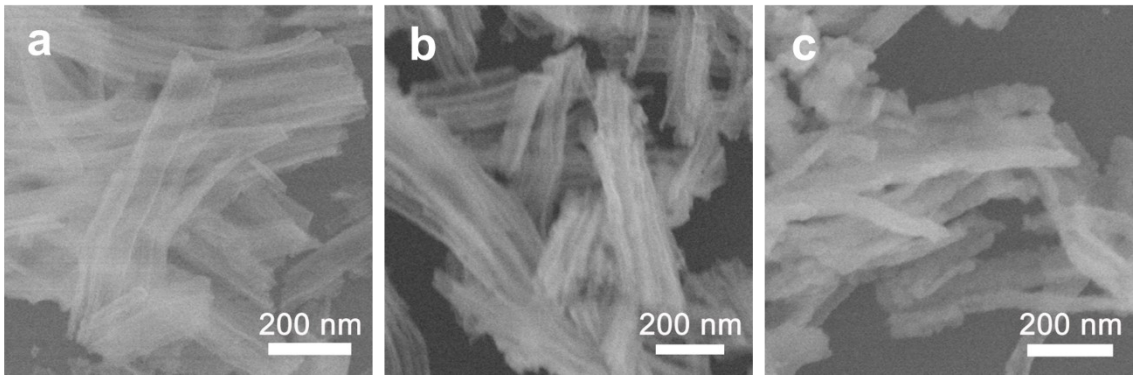

Figure S10. SEM images of (a) CeO_2-350-H_2, (b) CeO_2-500-H_2, and (c) CeO_2-700-H_2.

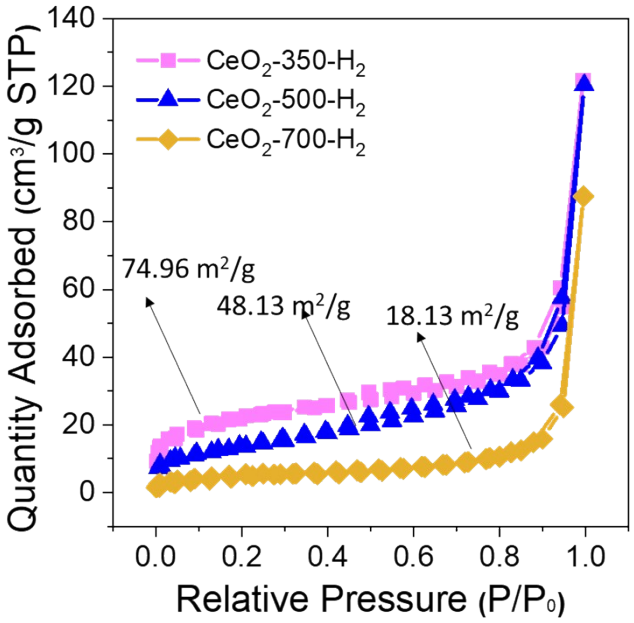

Figure S11. BET analysis of CeO_2-350-H_2, CeO_2-500-H_2, and CeO_2-700-H_2.

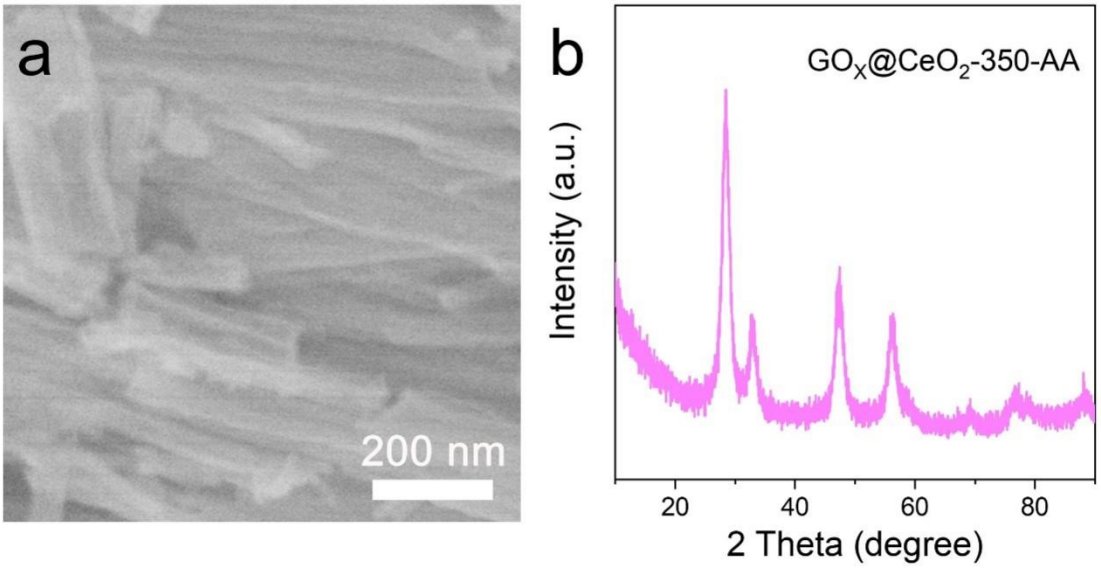

Figure S12. (a) The SEM images of GOx@ CeO_2-350-AA, (b) The XRD pattern of GOx@ CeO_2-350-AA.

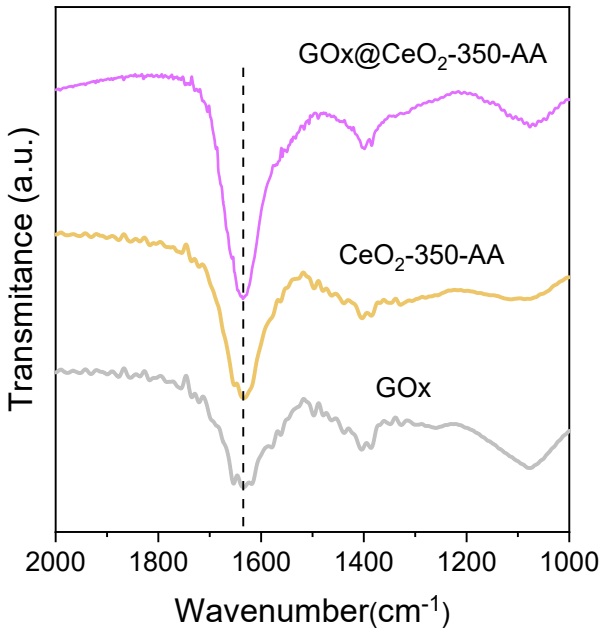

Figure S13. FT-IR spectroscopy of GOx, CeO_2-350-AA and GOx@CeO_2-350-AA.

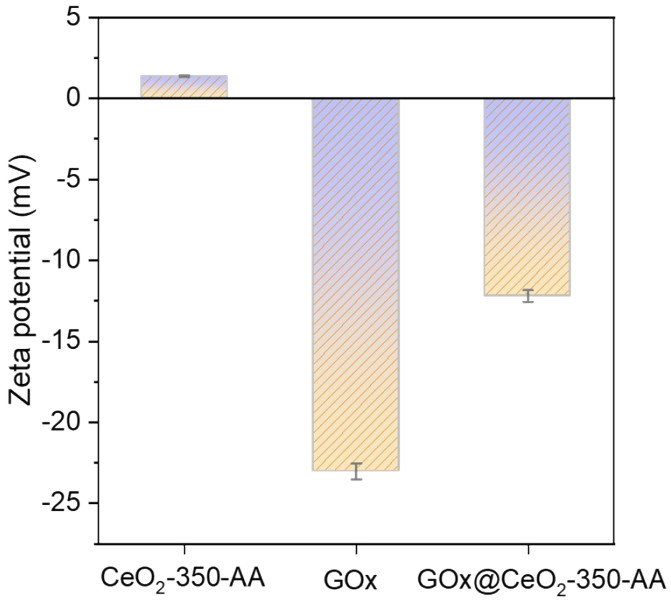

Figure S14. Zeta potentials of CeO_2-350-AA, GOx and GOx@CeO_2-350-AA.

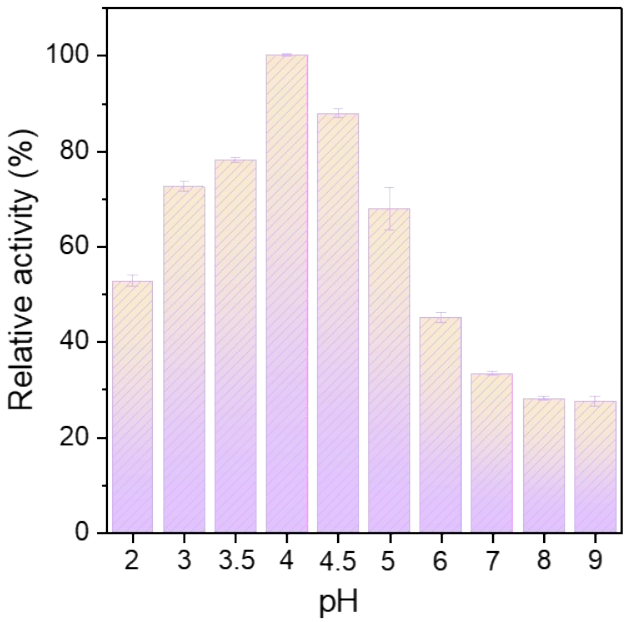

Figure S15. Influence of pH on the cascade reaction activity for GOx@CeO_2-350-AA.

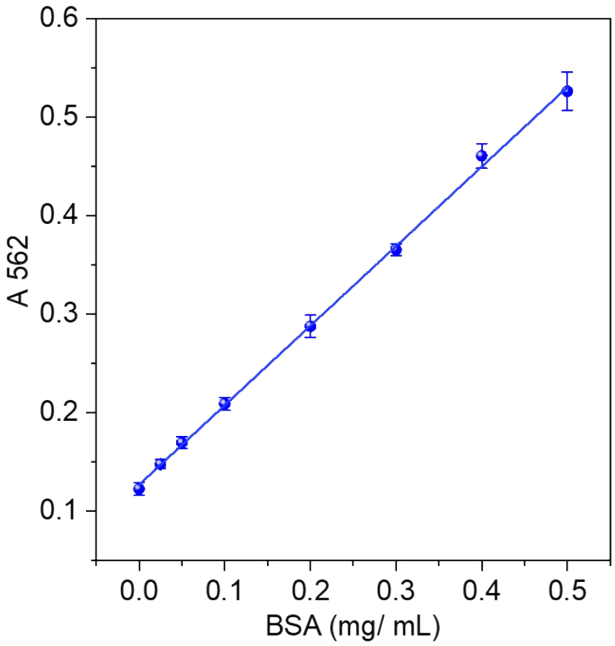

Figure S16. Standard curve of protein.

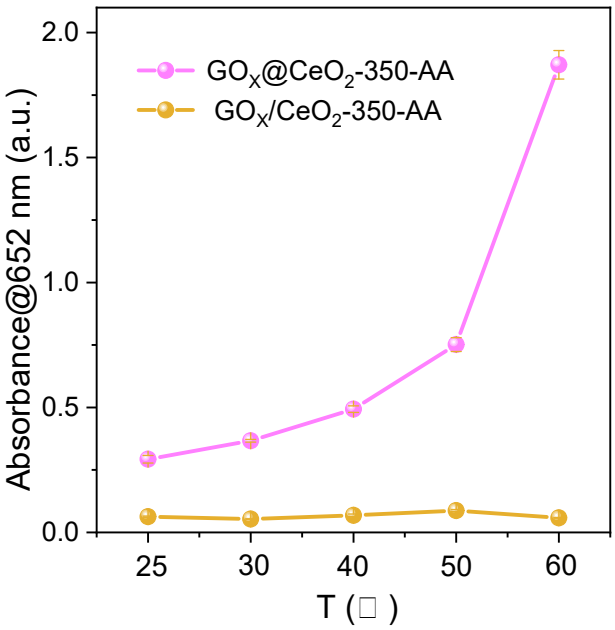

Figure S17. Effect of temperature on the peroxidase-like activity of GOx@CeO_2-350-AA and GOx/CeO_2-350-AA.

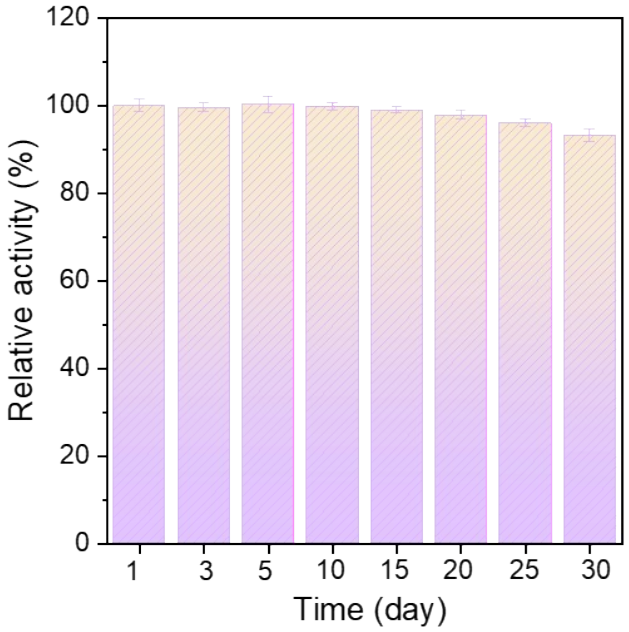

Figure S18. Relative activity of GOx@CeO_2-350-AA stored in a refrigerator at 5 °C for one month.

Table S1. Proportions of Ce^{3+} in different samples, which are simulated from XPS data.

sample	Ce^{3+}(%)
CeO_2-350	35.02
CeO_2-500	32.22
CeO_2-350-AA	43.48
CeO_2-350-H_2	32.86
CeO_2-500-H_2	31.75
CeO_2-700-H_2	31.18
CeO_2-$NaBH_4$	37.51

Table S2. The comparison of the kinetic parameters for POD-like activity.

nanozyme	substrate	K_m (mM)	V_{max} (M s^{-1})	*Ref.*
CeO_2-350-AA	H_2O_2	8.774	1.72×10^{-8}	This work
	TMB	0.397	2.64×10^{-8}	
CeO_2-350	H_2O_2	12.179	2.83×10^{-9}	
	TMB	1.881	9.09×10^{-9}	
CeO_2-TCPP	H_2O_2	3.86	6.67×10^{-8}	1
Ti_3C_2/CeO_2-PVP	H_2O_2	19.52	4.3×10^{-8}	2
Au@CeO_2	H_2O_2	0.007	8.26×10^{-9}	3
	TMB	0.061	1.51×10^{-9}	
Ce-BPyDC	H_2O_2	4.41	1.005×10^{-6}	4
	TMB	0.16	2.68×10^{-7}	
CeO_2-Cube	H_2O_2	41.6	1.16×10^{-9}	5
CeO_2-Sphere	H_2O_2	79.5	5.8×10^{-10}	
CeO_2 Cube	H_2O_2	30.9	3.45×10^{-9}	6
	TMB	0.1801	1.09×10^{-9}	

Table S3. Comparison of nanozyme-based biosensors for the detection of glucose.

Nanozyme	Linear range (μM)	Detection limit (μM)	Reaction time (min)	Ref.
GOx@CeO_2-350-AA	50-1000	9.3	10	This work
Fe-MOF-GOx	1-500	0.487	30	7
GOx@ZIF-8(NiPd)	10-300	9.2	60	8
GOx@ZIF-8@Fe-PDA	5-100	1.1	60	9
GOx@Fe (III)-BTC	5-100	2.4	60	10
GOx/hemin@ZIF-8	0-240	1.7	60	11
GOx@HP-MIL-88BBA	2-100	0.98	10	12

Reference：

1. W. Li, M. Qi, J. Zhou, Y. Sun, J. Sun, B. Dong, L. Wang and S. Song, Pathogen-Activated Macrophage Membrane Encapsulated CeO_2-TCPP Nanozyme with Targeted and Photo-Enhanced Antibacterial Therapy, *Small*, 2023, **20**, 2309664.

2. M. Tang, Y. Shi, L. Lu, J. Li, Z. Zhang, J. Ni, W. Wang, Y. Zhang, T. Sun and Z. Wu, Dual active nanozyme-loaded MXene enables hyperthermia-enhanced tumor nanocatalytic therapy, *Chem. Eng. J.,* 2022, **449**, 137847.

3. C. Liu, M. Zhang, H. Geng, P. Zhang, Z. Zheng, Y. Zhou and W. He, NIR enhanced peroxidase-like activity of Au@CeO_2 hybrid nanozyme by plasmon-induced hot electrons and photothermal effect for bacteria killing, *Appl. Catal. B: Environ.,* 2021, **295**, 120317.

4. L. Luo, L. Huang, X. Liu, W. Zhang, X. Yao, L. Dou, X. Zhang, Y. Nian, J. Sun and J. Wang, Mixed-Valence Ce-BPyDC Metal–Organic Framework with Dual Enzyme-like Activities for Colorimetric Biosensing, *Inorg. Chem.,* 2019, **58**, 11382-11388.

5. Z. Tan, Y. Wang, J. Zhang, Z. Zhang, S. S. Man Wong, S. Zhang, H. Sun, K. K. L. Yung and Y. K. Peng, Shape Regulation of CeO_2 Nanozymes Boosts Reaction Specificity and Activity, *Eur. J. Inorg. Chem.,* 2022, e202200202.

6. J. Zhang, Z. Tan, W. Leng, Y.-C. Chen, S. Zhang, B. T. W. Lo, K. K. L. Yung and Y.-K. Peng, Chemical state tuning of surface Ce species on pristine CeO_2 with 2400% boosting in peroxidase-like activity for glucose detection, *Chem. Commun.,* 2020, **56**, 7897-7900.

7. Xu, W.; Jiao, L.; Yan, H.; Wu, Y.; Chen, L.; Gu, W.; Du, D.; Lin, Y.; Zhu, C., Glucose Oxidase-Integrated Metal–Organic Framework Hybrids as Biomimetic Cascade Nanozymes for Ultrasensitive Glucose Biosensing. *ACS Appl. Mater. Interfaces,* 2019, **11**, 22096-22101.

8. Wang, Q.; Zhang, X.; Huang, L.; Zhang, Z.; Dong, S., GOx@ZIF-8(NiPd) Nanoflower: An Artificial Enzyme System for Tandem Catalysis. *Angew. Chem. Int. Ed.,* 2017, **56**, 16082-16085.

9. Zhao, Z.; Lin, T.; Liu, W.; Hou, L.; Ye, F.; Zhao, S., Colorimetric detection of

blood glucose based on GOx@ZIF-8@Fe-polydopamine cascade reaction. *Spectrochimica Acta Part A: Molecular and Biomolecular Spectroscopy,* 2019, **219**, 240-247.

10. Zhao, Z.; Pang, J.; Liu, W.; Lin, T.; Ye, F.; Zhao, S., A bifunctional metal organic framework of type Fe(III)-BTC for cascade (enzymatic and enzyme-mimicking) colorimetric determination of glucose. *Microchim. Acta,* 2019, **186**, 295.

11. Cheng, H.; Zhang, L.; He, J.; Guo, W.; Zhou, Z.; Zhang, X.; Nie, S.; Wei, H., Integrated Nanozymes with Nanoscale Proximity for in Vivo Neurochemical Monitoring in Living Brains. *Anal. Chem.* 2016, **88**, 5489-5497.

12. Zhao, Z.; Huang, Y.; Liu, W.; Ye, F.; Zhao, S., Immobilized Glucose Oxidase on Boronic Acid-Functionalized Hierarchically Porous MOF as an Integrated Nanozyme for One-Step Glucose Detection. *ACS Sustain. Chem. Eng.* 2020, **8**, 4481-4488.